Short-Time Electron Dynamics in Aluminum Excited by Femtosecond Extreme Ultraviolet Radiation

N. Medvedev,[1,2] U. Zastrau,[3] E. Förster,[3] D. O. Gericke,[4] and B. Rethfeld[1]

[1]*Fachbereich Physik und Forschungszentrum OPTIMAS, Technische Universität Kaiserslautern, Erwin-Schrödinger-Straße, 67663 Kaiserslautern, Germany*

[2]*Center for Free-Electron Laser Science, DESY, 22607 Hamburg, Germany*

[3]*Institut für Optik und Quantenelektronik, Friedrich-Schiller-Universität Jena, Max-Wien-Platz 1 und Helmholtz-Institut Jena, Helmholtzweg 4, 07743 Jena, Germany*

[4]*Centre for Fusion, Space and Astrophysics, Department of Physics, University of Warwick, Coventry CV4 7AL, United Kingdom*

(Received 3 April 2011; published 12 October 2011)

The femtosecond dynamics of the electrons in aluminum after an intense extreme ultraviolet pulse is investigated by Monte Carlo simulations. Transient distributions of the conduction band electrons show an almost thermalized, low-energy part and a high-energy tail. Constructing emission spectra from these data, we find excellent agreement with measurements. The radiative decay mainly reflects the colder part of the distribution, whereas the highly excited electrons dominate the bremsstrahlung spectrum. For the latter, we also find good agreement between predicted and measured energy scales.

DOI: 10.1103/PhysRevLett.107.165003 PACS numbers: 52.27.Gr, 52.65.−y, 78.47.J−

One of the most exciting regimes of matter is located between cold solids, with a long-range ion structure and degenerate electrons, and the ideal, classical plasma state [1]. Such warm dense matter (WDM) is of high interest to basic science, planetary and stellar astrophysics [2,3] and research towards inertial confinement fusion [4]. The creation of well-defined, homogeneous samples of WDM is demanding even in a state-of-the-art laboratory as the energy deposition is required to be both extremely rapid and uniform throughout the target. The diagnostics of WDM states is also challenging due to the high particle densities prohibiting the use of optical light [5–7].

Today brilliant 4th generation light sources for extreme ultraviolet (XUV, photon energies ∼100 eV) [8] and soft x-ray radiation [9] provide intensities that have hitherto remained the province of optical lasers. Having all the advantages of optical lasers, such as subpicosecond pulse durations and focused intensities of up to 10^{17} W/cm^2, the shorter wavelength enables the radiation to penetrate even highly ionized solid-density matter. Furthermore, the ponderomotive potential, responsible for the creation of multi-MeV electrons with optical lasers, scales as $I\lambda^2$ and does not exceed values of a few eV for XUV radiation. Finally, solids absorb XUV pulses dominantly via single-photon bound-free absorption.

These properties make light pulses from 4th generation light sources well suited for the creation and probing of WDM. Indeed, several publications reported on isochoric heating of matter by intense XUV pulses [10–12]. Taking aluminum as an example, one finds that the light-matter interaction is dominated by bound-free ionization of L states if the photon energy exceeds the L absorption edge of 73 eV. The M-shell electrons in the conduction band have a fairly small free-free absorption coefficient and the core electrons in the K shell are too tightly bound to contribute to the absorption of XUV light.

After excitation, nonradiative Auger recombination is the fastest decay process whereas only a small fraction of L-shell holes is filled radiatively [11–13]. However, this radiative decay reveals the structure of the conduction band. Present, time-integrated measurements yield data averaged over the first tens to hundreds femtoseconds since later all L-shell vacancies have recombined. The emitted light yields thus information on the electron properties in such exotic nonequilibrium states. Recent experiments on aluminum samples irradiated by ultrashort XUV radiation have however shown contradictory results: while the analysis of the Bremstrahlung emission suggested electron temperatures of approximately 40 eV [10], the L-shell radiative spectra were found to be in agreement with an electron Fermi distribution having a temperature of ∼1 eV only [12]. As both emissions occur on a femtosecond time scale, these significantly different temperatures raise serious questions.

In this Letter, we resolve the problem of the disagreeing electron temperatures reported in Refs. [10,12]. The key point for an understanding of these results is the short-time evolution of the electrons in the conduction band. Our time-resolved Monte Carlo simulations demonstrate that the combination of excitation, thermalization and prolonged energy deposition from Auger recombination creates an electron distribution consisting of a Fermi-like part and a low-density, but high-energy tail. The large number of electrons in the colder (Fermi) part dominates the radiative decay. Forward modeling yields very good agreement with the experimental XUV emission spectra [10–12]. The Bremsstrahlung spectra result, on the other hand, from energetic electrons. Considering the hot tail of

the calculated electron distribution only, we also find good agreement with the electron temperature inferred from the Bremsstrahlung spectrum [10]. The agreements with measured spectra demonstrate that the simulation model applied is a reliable tool to obtain the electron dynamics in highly excited solids.

To model the short-time electron dynamics in response to a femtosecond pulse, we apply a Monte Carlo scheme of event-by-event simulations [14–16]. This approach is a robust and stable tool to model nonequilibrium kinetics. It was developed to describe electronic excitations after an ion impact on dielectrics [16]. Further generalizations were successfully applied to semiconductors irradiated by ultrashort laser pulses [17] and metallic targets [18,19]. Our simulations take into account the density of states (DOS) for the given material and Pauli's principle. Here, we consider the following processes: photoabsorption by bound and free electrons, secondary impact ionization by free electrons, elastic scattering of electrons on target atoms or ions, scattering of two electrons in the conduction band, and Auger processes involving free electrons in the conduction band and holes in deep atomic shells.

The absorption of photons by bound and free electrons is described by a material-dependent attenuation length. The cross section for impact ionization of bound electrons is determined by an expression obtained by Gryziński [20], which depends only on the ionization potential of the electron. The scattering between two free electrons is described by a dynamically screened Coulomb potential within the Lindhard dielectric formalism, equivalent to the Lenard-Balescu equation, [15,21]. Strong scattering [22] is here of minor importance due to the high electron Fermi energies to be considered.

For the description of Auger processes filling holes in the L shell, we apply an exponential law for the time of decay with a material-dependent time constant [15,17]. The electrons involved in the Auger transition as well as the partners for free-free collisions are randomly chosen among the electrons in the conduction band.

Finally, all interaction probabilities are multiplied with a Pauli factor, $f_c(E_i)[1 - f_c(E_j)]$, where $f_c(E_i)$ is the distribution function of electrons at the energy level E_i and the term $[1 - f_c(E_j)]$ accounts for the probability of free places at the final energy level E_j. Thus, the second term ensures the Pauli principle after an electron has gained (or lost) the energy $(E_j - E_i)$. The dynamics of secondary electrons, produced by the first generation of the free electrons and holes, and their interactions were taken into account in the same manner. Further details of the numerical algorithm can be found in Refs. [16,17,19], a complete description of the method and the applied probabilities will also be available in a forthcoming publication [23].

We now apply our Monte Carlo scheme to model the interaction of solid aluminum (mass density: 2.7 g/cm^3, atomic density: $n_{\mathrm{at}} = 5.9 \times 10^{28}$ m^{-3}) with femtosecond XUV radiation. Considering homogeneous heating, we calculate a box of $10 \times 10 \times 10$ nm^3 with periodic boundary conditions. Energies are counted from the bottom of the conduction band yielding a Fermi energy of $E_F = 11.2$ eV and a L-shell location of -62 eV. The characteristic decay time for L-shell holes in aluminum is $t_A = 40$ fs [13,24].

At the start of the simulation, the electron distribution fills the conduction band up to Fermi energy ($T = 0$ K). The number of electrons per energy state accounts for the DOS of aluminum [25]. The parameters for the XUV pulse were chosen to mimic the details of experiments at the free-electron laser FLASH [10–12]. The temporal intensity envelope of the laser pulse has a Gaussian shape with a full width of half maximum duration of $\tau_L = 10$ fs with a maximum at 15 fs. The photon energy considered is $\hbar\omega = 92$ eV (wavelength of $\lambda = 13.5$ nm).

With these initial setups, we simulate the short-time evolution of the electrons now. Figure 1 presents snapshots

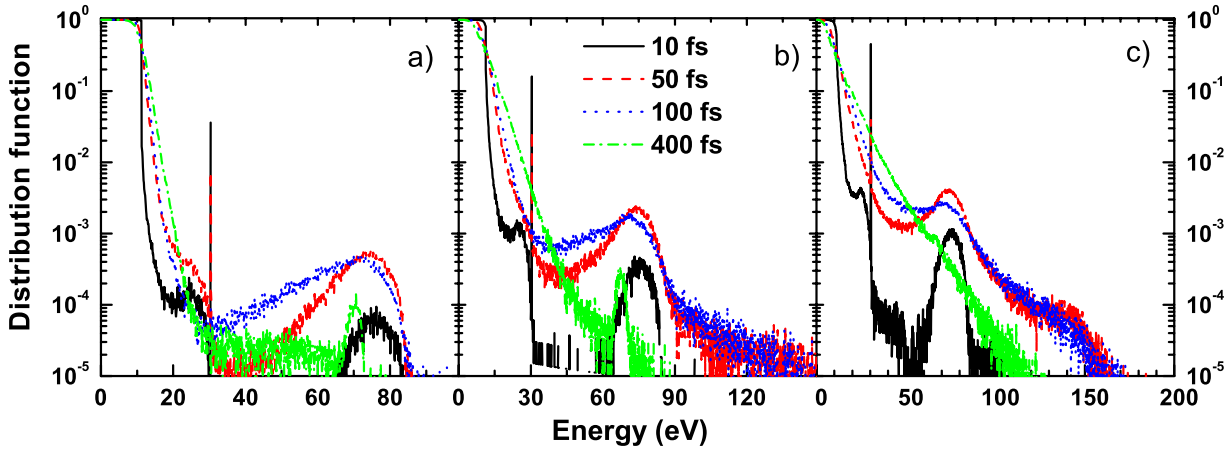

FIG. 1 (color online). Evolution of the electron distribution for different fluences of the XUV pulse (a) 0.2 J/cm^2, (b) 1.5 J/cm^2, and (c) 5 J/cm^2.

of the energy distribution function for the electrons in the conduction band of solid aluminum irradiated with total fluences of 0.2, 1.5, and 5 J/cm^2. At these relatively low fluences, the electronic structure is close to the one of cold aluminum [12]. Thus, the ground state models applied in our simulations are still applicable. For higher fluences, changes in the band structure and the scattering rates must be taken into account.

The transient electron distribution function typically consists of several parts: (i) the main bath of conduction band electrons which is only slightly disturbed from a Fermi function, but with a finite, time-dependent temperature; (ii) a deltalike peak at 30 eV formed by photoexcitation of L-shell electrons, which is only present during the XUV pulse and then quickly decays; (iii) the high-energy part of the Auger electrons at the energies of 73 eV $\pm$ E_F; and (iv) a high-energy tail for arising from photoabsorption of free electrons and scattering events. Note, that the data are scattered due to the statistics in the Monte Carlo procedure applied here.

Without an external energy input, the electrons would simply relax into a Fermi distribution function. However, the short-time dynamics is here driven directly by photoabsorption and indirectly via the Auger processes. After the excitation of an electron into the high-energy states, this electron redistributes its energy by interacting with other conduction band electrons. This gives a rise to the tail of the distribution present at later times. For high fluences, this tail is also fed by conduction electrons that have absorbed a XUV photon. Only at a second stage, the highly energetic electrons tend to thermalize with the undisturbed electron bath raising its temperature and establishing a common Fermi distribution. However, this thermalization takes a relatively long time: for the high fluence of 5 J/cm^2, the distribution reaches a Fermi-like shape after approximately 400 fs. For lower fluences, a nonequilibrium tail with a bump at around 73 eV is present during the entire simulation time.

An analysis of the relaxation process reveals several, of course interconnected, stages which can be seen best when considering the entropy of the electron subsystem. During the first 30 fs the entropy sharply increases due to direct energy deposition of the XUV photons. Auger decays lead to a further strong increase over the following 200–250 fs. Afterwards, the entropy grows only slightly, reflecting the thermalization process in the electron subsystem on a timescale of about 400 fs. Finally, it slowly decreases when the energy transfer from the electrons to the lattice dominates. The results in Fig. 1 show that the time of Auger heating is (i) much longer than the relaxation time for free electrons with energies near the Fermi edge and (ii) significantly shorter than the time the high-energy electrons need to equilibrate. As long as both relations hold, our conclusions remain independent of the model applied for the scattering cross sections.

Our Monte Carlo simulations yield the evolution of the distribution function, $f_c(E, t)$, for the electrons in the conduction band and, via the DOS of aluminum, the number of electrons in a particular energy state at each time. This information can be used to calculate emission spectra of XUV excited aluminum. For that goal, we trace the electron distribution until all L-shell holes are decayed. At each event of radiative decay, we save the current distribution of electrons and, using the DOS, we obtain energy-dependent radiation probabilities. These results are added and normalized to yield the equivalent of a time-integrated spectrum. Finally, we convolute our numerical results with the point-spread function of the spectrometer used [11,12]. Performing this procedure for the four photon fluxes considered here enables us to compare measured and theoretically predicted data with outstanding accuracy.

Figure 2 compares the experimental spectra with the ones calculated by the procedure described above. Both sides of the spectra, which are dominated by the DOS and the distribution function, respectively, are described very well by our simulations. The very good agreement between experiment and theoretical model demonstrates the capabilities of the Monte Carlo scheme presented.

In contrast to the nonequilibrium analysis presented, the experimental emission spectra were also successfully modeled assuming equilibrium distributions [12], where the electron temperature was taken as a fit parameter. Indeed, the data presented in Fig. 2 look like spectra from thermalized systems although our simulations, see Fig. 1, show that the electrons have not established equilibrium distributions at times when all holes in the L shell have decayed. This seeming contradiction is resolved by the fact that the emission spectra highlight the part of the distribution where the majority of electrons are located. As most electrons have energies below and slightly above the Fermi energy, the emission spectra are very sensitive to the low-energy part of electron distribution. For these low energies,

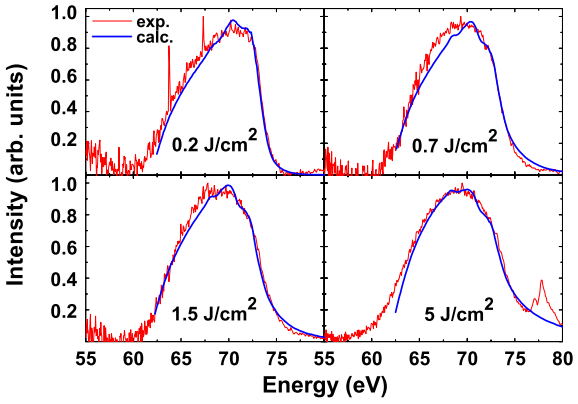

FIG. 2 (color online). Emission spectra for the conduction band to L-shell transition in aluminum irradiated by an XUV pulse (see text) for different fluences. Experimental data (thin spiky lines) are compared with calculated spectra (bold blue lines).

the nonequilibrium electron distribution is very close to a Fermi function and, thus, the calculated spectra appear equilibriumlike. The few electrons in the high-energy tail have, on the other hand, only a negligible effect on the theoretical emission spectra in Fig. 2.

To verify these arguments, we estimated an effective temperature for the high-density, low-energy part of the distribution. Fitting our nonequilibrium results with a Fermi functions yields a temperature close to 1 eV which is in very good agreements with the analysis based on equilibrium distributions [12]. This agreement does not imply however that such an equilibrium analysis is always appropriate as the high-energy tail can strongly influence other properties [26]. For instance, the obtained temperature of 1 eV strongly underestimates the energy content in the electron subsystem. Eventually, the energy in the hot tail will raise the temperature of the majority of electrons as well as the lattice or ion temperature, a process of great importance for WDM physics [27].

Information about the high-energy part of the electron distribution is contained in the Bremsstrahlung spectra from heated matter. Indeed, measurements on aluminum (conditions as for the emission spectra shown in Fig. 2) cannot be explained by the low temperature of 1 eV [10]. Boltzmann fits to the experimental spectra yield instead temperatures around 40 eV. Although carrying quite an error, this discrepancy is large enough to predict totally different systems: whereas electrons at 1 eV are highly degenerate, 40 eV would allow for a classical description.

To resolve this problem we have performed a separate analysis of the high-energy part of the nonequilibrium distributions shown in Fig. 1. First, we subtract the low-energy, Fermi-like part of each distribution function. The remaining high-energy part is averaged over time until thermalization to mimic a time-integrated measurement. Equating electron density and energy content of the hot tail by an equivalent Fermi function ($E = 3k_BT/2$ for nondegenerate electrons) yields an effective temperature of approximately 20 eV. This temperature agrees with the one extracted from the measured bremsstrahlung spectra within error bars [10]. Thus, nonequilibrium description of the electron properties of aluminum irradiated by a short, intense pulse of XUV radiation proved to be inevitable for a modeling of the Bremsstrahlung spectra.

In conclusion, we have investigated the dynamics of the electrons in aluminum during and after irradiation with a femtosecond pulse of 92 eV photons. Our analysis is based on a Monte Carlo scheme including all relevant excitation, decay and scattering processes. Particularly important are the band structure of the material, Pauli's principle, and Auger recombination of the L-shell holes. The nonequilibrium distributions obtained consist of a low-energy, Fermi-like branch and a nonthermalized high-energy tail. During the decay of the L-shell holes, Auger electrons result in an additional bump at 73 eV.

To benchmark the simulations, we have calculated spectra due to radiative decay of the L-shell holes and bremsstrahlung from the electron distributions obtained. The emission spectra show an excellent agreement with measured data. These data are most sensitive to the low-energy part of the distribution which can be modeled by a Fermi distribution with a temperature of 1 eV. The hot tail of the electron distribution can on the other hand explain the high temperatures that are needed to fit the experimentally obtained bremsstrahlung spectra. Thus, the full nonequilibrium electron dynamics is required to consistently describe both measured spectra which seem contradictory when being analyzed under the assumption of thermodynamic equilibrium. Our analysis has shown that the different temperatures obtained in Refs. [10,12] just reflect the (mean) energy contained in different parts of the nonequilibrium distribution function.

Our results demonstrate that nonequilibrium physics can play a key role when describing heating or probing of matter with ultrashort light pulses. Simulation tools for the short-time dynamics of the electrons will thus play a crucial role in further investigations.

The authors thank Sam Vinko (Oxford) and Georg Lefkidis (Kaiserslautern) for helpful discussions. Data for comparisons were obtained at FLASH within the Peak Brightness Collaboration. We also acknowledge financial support by grants from BMBF (FSP 301-FLASH), the DFG within Emmy Noeter program (RE 1141/11-1), and the UK's EPSRC (EP/D062837).

[1] R. W. Lee *et al.*, J. Opt. Soc. Am. B **20**, 770 (2003).
[2] N. Nettelmann *et al.*, Astrophys. J. **683**, 1217 (2008).
[3] B. Militzer *et al.*, Astrophys. J. Lett. **688**, L45 (2008).
[4] O. L. Landen *et al.*, Rev. Sci. Instrum. **72**, 627 (2001).
[5] S. H. Glenzer *et al.*, Phys. Rev. Lett. **90**, 175002 (2003).
[6] E. Garcia Saiz *et al.*, Nature Phys. **4**, 940 (2008).
[7] A. Pelka *et al.*, Phys. Rev. Lett. **105**, 265701 (2010).
[8] W. Ackermann *et al.*, Nat. Photon. **1**, 336 (2007).
[9] P. Emma *et al.*, Nat. Photon. **4**, 641 (2010).
[10] U. Zastrau *et al.*, Phys. Rev. E **78**, 066406 (2008).
[11] B. Nagler *et al.*, Nature Phys. **5**, 693 (2009).
[12] S. M. Vinko *et al.*, Phys. Rev. Lett. **104**, 225001 (2010).
[13] O. Keski-Rahkonen and M. O. Krause, At. Data Nucl. Data Tables **14**, 139 (1974).
[14] I. Plante and F. A. Cucinotta, New J. Phys. **11**, 063047 (2009).
[15] A. F. Akkerman *et al.*, Nucl. Instrum. Methods Phys. Res., Sect. B **227**, 319 (2005).
[16] N. Medvedev *et al.*, Phys. Rev. B **82**, 125425 (2010).
[17] N. Medvedev and B. Rethfeld, New J. Phys. **12**, 073037 (2010).
[18] N. Medvedev and B. Rethfeld, AIP Conf. Proc. **1278**, 250 (2010).
[19] N. Medvedev and B. Rethfeld, Proc. SPIE Int. Soc. Opt. Eng. **8077**, 80770Q (2011).

[20] M. Gryziński, Phys. Rev. **138**, A305 (1965); Phys. Rev. **138**, A322 (1965); Phys. Rev. **138**, A336 (1965).
[21] M. D. Barriga-Carrasco, Phys. Rev. E **82**, 046403 (2010).
[22] D. O. Gericke *et al.*, Phys. Rev. B **59**, 10 639 (1999).
[23] N. Medvedev *et al.*, Phys. Rev. E (to be published).
[24] C.-O. Almbladh, A. L. Morales, and G. Grossmann, Phys. Rev. B **39**, 3489 (1989).
[25] F. Ladstädter *et al.*, Phys. Rev. B **70**, 235125 (2004).
[26] D. A. Chapman and D. O. Gericke, Phys. Rev. Lett. **107**, 165004 (2011).
[27] J. Vorberger *et al.*, Phys. Rev. E **81**, 046404 (2010).